

# Nucleation of Spontaneous vortices in trapped Fermi gases undergoing a BCS-BEC crossover

A. Glatz,<sup>1</sup> H. Roberts,<sup>2,3</sup> I. S. Aranson,<sup>1</sup> and K. Levin<sup>2</sup>

<sup>1</sup>*Materials Science Division, Argonne National Laboratory, 9700 S. Cass Av., Argonne, IL 60439, USA*

<sup>2</sup>*James Franck Institute and Department of Physics, University of Chicago, Chicago, IL 60637, USA*

<sup>3</sup>*Physics Department, University of California, Berkeley, CA 94720, USA*

(Dated: June 2, 2019)

We study the spontaneous formation of vortices during superfluid condensation in a trapped fermionic gas subjected to a rapid thermal quench via evaporative cooling. Our work is based on the numerical solution of the time dependent crossover Ginzburg-Landau equation coupled to the heat diffusion equation. We quantify the evolution of condensate density and vortex length as a function of a crossover phase parameter from BCS to BEC. The more interesting phenomena occur somewhat nearer to the BEC regime and should be experimentally observable; during the propagation of the cold front, the increase in condensate density leads to the formation of supercurrents towards the center of the condensate as well as possible shock-wave generation.

PACS numbers: 67.85.-d, 67.85.De, 67.85.Jk, 74.20.De

The character and formation of spontaneous vortices in superfluids is of great interest to a number of different physics subdisciplines. These include the atomic physics investigations of trapped quantum gases [1, 2], cosmological theories which address the Kibble Zurek mechanism [3], as well as studies of homogeneous superfluids [4, 5] and high temperature superconductors [6–8]. With the Fermi gases and cuprate superconductors has come an additional opportunity to explore a tuneability of vortices and their dynamics associated with the crossover between the BCS (where the inter-fermionic attraction is weak) and the Bose-Einstein condensed (BEC) limits (where the attraction is strong). It has been argued [9] that the short coherence length of the cuprates, as well as the existence of high transition temperatures suggests that these systems are mid-way between BCS and BEC. Similarly, in the ultracold Fermi gases this crossover is entirely accessible through the exploitation of so-called Feshbach resonances [10, 11].

It is the goal of this Letter to investigate the character and time evolution of spontaneous vortices (which appear in the absence of magnetic fields) in Fermi superfluids. Our studies address the entire crossover from BCS to BEC and our vortices are created upon a rapid quench from the normal phase. Theoretical investigations of rapid quenches have been undertaken [1] for atomic Bose gases and appear consistent with experiments. It is of additional interest to compare our findings in the BEC limit of the composite boson or fermionic superfluid with these counterpart studies. It appears entirely feasible to conduct such experiments in future for the Fermi gases.

Our work is based on a numerical simulation of a time dependent Ginzburg-Landau type equation [12, 13]. We simulate the time-dependent *crossover* Ginzburg-Landau equation (TCGLE) in the presence of thermal (white) noise  $\chi$ . The effects of the BCS-BEC crossover enter primarily into the dynamics [10, 14] which is pure dissipative

in the BCS limit and energy-conserving in the BEC limit. We capture this feature by introducing a “crossover phase parameter”  $\theta = 0 \dots \pi/2$  that *tunes* the equation from the regular Ginzburg-Landau equation ( $\theta = 0$ , BCS) to the Gross-Pitaevskii equation ( $\theta = \pi/2$ , BEC). Interestingly, the variation in coherence length from BCS to BEC is found to play a relatively small role and, thus, we do not consider it. The TCGLE is given by

$$e^{i\theta} \partial_t \psi = A[\mathbf{r}, T(\mathbf{r}, t)] \psi - |\psi|^2 \psi + \frac{1}{2} \nabla^2 \psi + \chi(\mathbf{r}, t) \quad (1)$$

where  $\psi = \psi(\mathbf{r}, t)$  is the order parameter and  $\chi \in [-T_\chi; T_\chi]$  is uniformly distributed thermal noise with fluctuation temperature  $T_\chi$ .

The coefficient  $A[\mathbf{r}, T(\mathbf{r}, t)]$  takes into account the evaporative cooling of the system and the trapping potential, i.e.  $A[\mathbf{r}, T(\mathbf{r}, t)] = [1 - T(r, t)] - U_0/r^2$ , where  $U_0$  is the trapping potential which is determined by the trap size. Eq. (1) is written in dimensionless units, with length scale  $\xi_0$ , time scale  $\tau_0$ , and the order parameter scale  $\psi_0$ . Temperatures are measured in units of  $T_c$ . For (fermionic) Li<sup>6</sup> these values are estimated as:  $\xi_0 = 3.2 \cdot 10^{-6} \text{m}$ ,  $\tau_0 = 1.1 \cdot 10^{-2} \text{s}$ , and concentration  $\psi_0^2 = 2.9 \cdot 10^{16} \text{m}^{-3}$ . The dimensionless fluctuation temperature for a condensate at 10nK is in the interval  $T_\chi \in [0.02; 0.1]$ , depending on the condensed atoms.

The trap is assumed to be spherically-symmetric. Thus we calculate the temperature profile  $T(r, t)$  due to evaporative cooling by solving the spherically-symmetric heat diffusion equation

$$\partial_t T(r, t) = \mathcal{D} \left( \partial_r^2 + \frac{2}{r} \partial_r \right) T(r, t), \quad (2)$$

with an initial uniform temperature  $T(r < R, t = 0) = T_0$  and final temperature  $T(r \geq R, t) = T_f$  that is fixed at

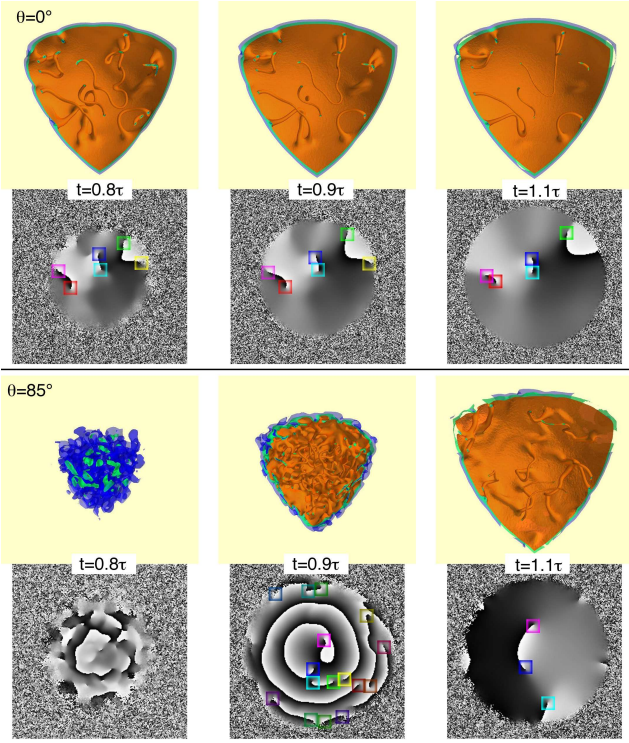


FIG. 1. (Color online) Isosurfaces and phase-cuts of the order parameter at different times. The upper row shows the 3D isosurfaces for the BCS ( $\theta = 0$ ) case at times  $t = 0.8\tau, 0.9\tau, 1.1\tau$ , where  $\tau$  is the time needed to reach half of the condensate steady state volume [see Fig. 2 (top)]. The phase-cuts (phase  $\varphi = \arg \psi$ ) are cuts through the center in the  $xy$ -plane - vortices are marked as the end-points of  $2\pi$ -phase jump lines (sharp black-white transition). The lower row shows the same pictures, but towards the BEC limit represented by  $\theta = 85^\circ$ .

the boundary  $r = R$ . The heat diffusion constant  $\mathcal{D}$  is renormalized by  $\xi_0^2/\tau_0$ ; typical values for Li<sup>6</sup>:  $\mathcal{D} \simeq 3$ .

All simulation runs start with random initial conditions in the normal phase ( $|\psi|^2 \ll 1$ ) at temperatures  $T_0$  larger than the critical temperature  $T_c$ . The evaporative cooling is initiated at time  $t = 0$  on the surface of our spherical trap with radius  $75\xi_0$ . The cold front surface propagates towards the center and quenches the atomic gas below the critical temperature. The dimensionless diffusion constant was typically set to  $\mathcal{D} = 10$  and the fluctuation strength  $T_\chi = 0.02$ . This mechanism of condensate nucleation is to be contrasted with that described in Ref. [1] where the cooling occurred uniformly in space, thus corresponding to an infinite diffusion constant. Another crucial difference with this previous work is the equilibration mechanism: the time evolution of the condensate used in [1] was based on the Gross-Pitaevskii model where the dissipation was introduced by truncation of high-frequency modes. By contrast, our TCGLE model includes a complex relaxation rate which is determined by the crossover physics through the phase factor  $e^{i\theta}$ . Experiments on these cold gases [10] cannot probe

very deeply into the BCS or BEC regimes, but are confined to the so-called “unitary” midpoint. Nevertheless, at unitarity, pairs are reasonably long lived [14] so that we can associate  $\theta \approx 70^\circ - 85^\circ$  with the physically accessible regime.

Our numerical calculations were done for volumes discretized in up to  $512^3$  grid points, averaged over up to 50 different initial conditions and time evolved for 65 different crossover phase values. The timestep in dimensionless units was chosen to be 0.1 and the total simulation time up to 3000 at  $\theta$ -values close to the BEC limit. Our quasi-spectral split step method to solve the TCGLE which uses fast Fourier transforms, is much more stable than the traditional finite difference method. Compared to recent works [1], our systems are an order of magnitude larger which is a consequence of employing modern graphics processing units (we used a cluster of Nvidia Tesla C2050/2070 cards) that provided a speed-up of our simulations by up to a factor 100 compared to traditional CPU-based computations.

We begin with an illustration of the time evolved condensation process for the BCS limit ( $\theta = 0$ ) and a near-BEC situation ( $\theta = 85^\circ$ ). Throughout this paper we avoid the strict fermion-based BEC limit ( $\theta = \pi/2$ ) since without dissipation the condensate does not form and nucleation of vortices is completely suppressed. By introducing a complex relaxation rate in the TCGLE, we avoid having to include the interactions between condensed and non-condensed pairs which do not enter as naturally, in the fermionic- BEC limit. These were essential for addressing the bosonic counterpart experiments [1, 15].

Plotted in Fig. 1 are the isosurfaces for constant condensate magnitude. We also show cross-sections in the  $xy$ -plane through the center of the system, indicating the phase of the order parameter  $\varphi = \arg \psi$ . These latter plots appear below the counterpart isosurface pictures and contain information about spontaneous vortices. The isosurfaces for the condensate magnitude are color-coded according to fixed condensate density values  $\rho_s \equiv |\psi|^2$ , where we used  $\rho_s = 0.1, 0.2, 0.3$ . The three different panels from left to right correspond to three different times close to the typical time  $\tau$  at which the condensate forms, i.e. the time when the condensate volume reaches half of its saturation value.

One can see from Fig. 1, that most spontaneous vortices are connected to the surface of the condensate. Their time evolution is entirely accessible in our simulations [16] and one can follow their decay in the bulk and at the condensate surface. In the phase cross-section plots, these vortices are even more visible appearing as topological defects (phase singularities). Although vortices are most plentiful at the surface of the condensate, we find their decay occurs mostly in the bulk.

It is clear that in the BCS limit the condensate forms quickly occupying the entire trap volume in a relatively short time period. At much longer time scales (than

shown here), the condensate will appear uniform. The near-BEC limit exhibits an interesting contrast: Here the condensate expands slowly, and vortices are much more plentiful, decaying even more gradually. An interesting feature is shown in the middle panel of the last row of Fig. 1. We observe in the course of condensate formation, concentric rings in the phase cross-section interrupted by trapped topological defects. This corresponds to the generation of supercurrents from the surface of the condensate towards its center. The phenomenon of transient supercurrent  $\mathbf{J}_s = \rho_s \nabla \varphi$  generation can be understood as follows: In the BEC limit the TCGLE can be written in the hydrodynamic form [17] with the condensate density  $\rho_s$  satisfying the continuity equation  $\partial \rho_s / \partial t = -\nabla \cdot \mathbf{J}_s$ . During the quench,  $\rho_s$  changes from zero to its maximal value leading to the formation of supercurrents.

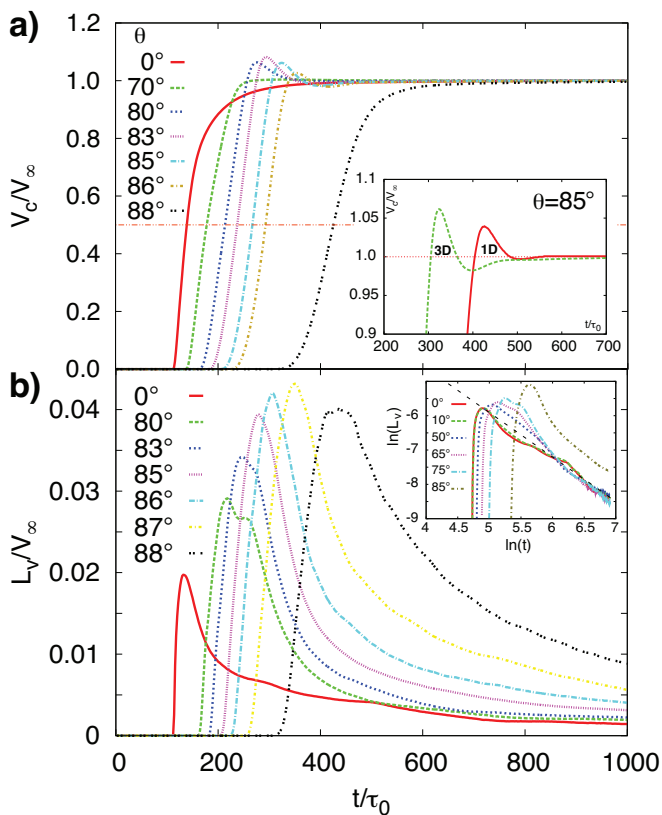


FIG. 2. (Color online) a) Condensate volume  $V_c/V_\infty$  normalized to the asymptotic condensate volume  $V_\infty$  with simulation time  $t/\tau_0$  for different crossover phases  $\theta$ . The horizontal line at  $V_c/V_\infty = 1/2$  can be used to read the typical condensate formation time  $\tau$ . Inset: the behavior of the condensate volume near the “overshoot” for  $\theta = 85^\circ$  for the full simulation (labelled 3D) and the spherically-symmetric equation (labelled 1D). b) Time evolution of the vortex length  $L_v/V_\infty$  for different  $\theta$ . Inset: a log-log representation illustrating a power-law decay for different  $\theta$ . The straight dashed line corresponds to a  $1/t$  decay.

condensate volume  $V_c$ , as well as the vortex length  $L_v$  for different values of the crossover phase  $\theta$ . Both quantities are normalized to the asymptotic final condensate volume. Here the condensate volume is calculated from the number of grid points with condensate density larger than 0.2. Assuming a spherical shape of the condensate (reflecting the trapping potential) we establish the diameter of the condensate; we then calculate the number of grid points with  $\rho_s < 0.2$  inside this sphere to estimate the vortex length. In the BCS limit the dissipation is maximum which is responsible for the rapid formation of the condensate. Increasing  $\theta$  as one approaches the near-BEC gradually delays the formation of the condensate leading to increase of the maximum total vortex length.

The vortices show a roughly  $1/t$ -decay of the total vortex length [2, 3]. In Fig. 2b the time dependence of the total vortex length is plotted from the BCS to the near-BEC limit. The inset shows some of these same curves on a log-log scale and compares with a linear curve (dashed) representing a  $1/t$  decay. In two dimensions, bulk vortices annihilate in pairs, the relaxation should be proportional to the square of the vortex concentration, i.e. the relaxation follows a power-law [18]. Similarly, a  $1/t$  is expected for the decay of vortex lines in 3D for the BCS case and  $1/t^{3/2}$  near the BEC limit [19]. The deviations from  $1/t$  power law are likely caused by finite size effects.

The condensate volume shows a well pronounced overshoot with subsequent oscillations in time. This occurs at intermediate values of the cross-over phase closer to the BEC limit. We quantify this “shock wave” effect by studying the height of this condensate volume overshoot in the inset of Fig. 3. Plotted here is the maximum of the volume of the condensate as a function of  $\theta$ . Also indicated is the maximum vortex length within the condensate. It can be seen that the maximum of the condensate overshoot occurs at  $\theta = 82.5^\circ$ . Near the BCS limit, the dissipation of the system is large and there is no “overshoot”. In the near-BEC limit, the dissipation is strongly suppressed and the condensate takes longer to form than the time associated with a thermal quench. The appearance of the overshoot is also characterized by the time scale  $t_{c,\max}$ , where the condensate reaches its maximum, which diverges below  $\theta \sim 60^\circ$  (since there is no overshoot) and near the BEC limit (because the time of the occurrence of the overshoot diverges for  $\theta \rightarrow \pi/2$ ). A minimum of  $t_{c,\max}$  is observed at  $75^\circ$ , i.e., the overshoot happens fastest. Fig. 3 indicates the typical time scale of the condensate formation  $\tau$  and the nearly identical time scale  $t_{v,\max}$ , which is the time at which the vortex length is maximum. Both these times generally depend only weakly on  $\theta$ , except near  $\theta \rightarrow \pi/2$ . Also the typical decay time of the vortices  $t_{v,\text{decay}}$  appears to be nearly independent of  $\theta$  below  $\sim 85^\circ$  (see Fig. 2b). Using the experimental time scales for  $\text{Li}^6$ , we can conclude from Fig. 2 and Fig. 3, that the condensate forms within a few seconds and on the same time scale vortices

Fig. 2 presents a plot of the time evolution of the con-



annihilate.

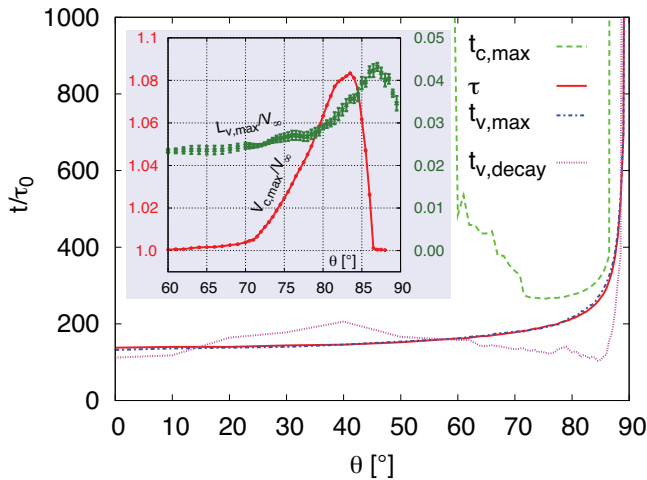


FIG. 3. (Color online) Time scales extracted from the time evolution of the condensate volume and vortex length [time in units of  $\tau_0$ ].  $\tau$  is the time needed to reach half of the steady state condensate volume.  $t_{c,max}$  and  $t_{v,max}$  are the times when the condensate volume and vortex length has a local maximum respectively.  $t_{v,decay}$  is the time over which the vortex length decays to  $1/e$  of its maximum value. Inset: Maximum of the volume of the condensate  $V_{c,max}$  and vortex length  $L_{v,max}$  normalized to  $V_\infty$  versus the crossover phase  $\theta$ . The data is thermally averaged over 10 to 50 realizations.

The overshoot and subsequent time oscillations of the condensate may be related to excitation of sound waves produced in a spherical trap by the quench. To further clarify this phenomenon we solved the spherically-symmetric TCGLE and obtained similar behavior as shown in the inset to Fig. 2a; the main difference being a delay in the condensate nucleation [20]. In the process we verified that the period of these oscillations is close to the time needed for sound waves to traverse the condensate. Indeed in our units the speed of sound (which emerges from the BEC limit of the TCGLE) is equal to unity in the long-wavelength limit, while the oscillation period obtained from Fig. 2a is approximately 140 time units. This is close to the time needed for the sound wave to cross our system with diameter 150 length units. Using the value for  $\xi_0$  and  $\tau_0$  for  $\text{Li}^6$ , the speed of the second sound is on the order  $10^{-4}\text{m/s}$ , comparable to the mean velocity of the atoms at 10nK.

Among the most exciting opportunities afforded by the ultracold Fermi gases is the possibility of addressing non-equilibrium phenomena, as we do here, such as the spontaneous formation of topological defects after a quench. We argue that our simulations correspond to entirely feasible Fermi gas experiments; although the quenches cannot be done instantaneously, one can follow the protocols in Ref. 1. Indeed, because losses due to three body collisions are suppressed, due to the Pauli principle, this makes it possible to study these quenches of Fermi gases

in the strong interaction regime. For the Bose counterparts, collisions are more problematic and restrict consideration to weaker interaction strengths. That our systems exhibit complex relaxation dynamics leads to a rich array of phenomena. As a function of the continuous crossover from BCS to BEC we see that the number and lifetime of spontaneous vortices increases, so that the steady state condensate is slower to form. Some of the most visible and striking behavior is found on the BEC-side of the crossover. During the propagation of the cold front, the increase in condensate density leads to the formation of supercurrents towards the center of the condensate. In addition we observe a shock-wave generation during the quench leading to an *overshoot* of the condensate volume. Cosmological implications of these rapid quenches have been viewed as an important motivation. Our work, albeit for an inhomogeneous case, shows how the trapped Fermi gases can add to our understanding of non-equilibrium phase transitions and, possibly, the Kibble Zurek mechanism.

We thank Kara Lamb, Matt Davis, Chih-Chun Chien and Nate Gemelke for useful discussions. This work was supported by the U.S. DOE, Office of Basic Energy Sciences, Division of Materials Science and Engineering, under Contract DEAC02-06CH11357, and by NSF-MRSEC Grant No. 0820054 (KL).

- 
- [1] C. N. Weiler *et al.*, Nature **455**, 948 (2008).
  - [2] N.G. Berloff and B.V. Svistunov, Phys. Rev. A **66**, 013603 (2002).
  - [3] N.D. Antunes, L.M.A. Bettencourt, W.H. Zurek, Phys. Rev. Lett. **82**, 2824 (1999).
  - [4] C. Bauerle *et al.*, Nature (London) 382, 332 (1996).
  - [5] V.M.H. Ruutu *et al.*, Nature (London) 382, 334 (1996)
  - [6] Y. Wang, Z. Xu, T. Kakeshita, S. Uchida and N. P. Ong, Phys. Rev. B. **64**, 224519 (2001).
  - [7] R. Carmi, E. Polturak, G. Koren, and A. Auerbach, Nature **404**, 853 (2000).
  - [8] A. Maniv, E. Polturak and G. Koren, Phys. Rev. Lett. **91**, 197001 (2003).
  - [9] A. J. Leggett, Nature Physics **2**, 134 (2006).
  - [10] Q.J. Chen, J. Stajic, S. Tan and K. Levin, Phys. Rep. **412**, 1 (2005).
  - [11] M. Zwierlein, C. Schunck, A. Schirotzek, W. Ketterle, Nature **442**, 52 (2006).
  - [12] I. S. Aranson, N. B. Kopnin, and V. M. Vinokur, Phys. Rev. Lett. **83**, 2600 (1999); Phys. Rev. B **63**, 184501 (2001)
  - [13] I. Aranson, L. Kramer, Rev. Mod. Phys. **74**, 99 (2002).
  - [14] J. Maly, B. Jankó, and K. Levin, Physica C **321**, 113 (1999).
  - [15] A.S. Bradley, C.W. Gardiner, and M.J. Davis, Phys. Rev. A **77**, 033616 (2008).
  - [16] Supplementary information and movies can be found at PROLA or <http://mti.msd.anl.gov/highlights/bcsbec>.
  - [17] T. Frisch, Y. Pomeau and S. Rica, Phys. Rev. Lett. **69**,

- 1644 (1992).
- [18] W. F. Vinen, Proc. R. Soc. London A **242**, 493 (1957)
  - [19] M. Kobayashi and M. Tsubota, J. Low Temp. Phys, **145**, 209 (2006)
  - [20] The spherically-symmetric TCGLE cannot capture the

full dynamics and does not admit vortex solutions because of the reduced dimensionality. Correspondingly the noise amplitude is reduced and becomes a function of the distance from the center of the condensate.